IEEE Access
Multidisciplinary | Rapid Review | Open Access Journal

Received May 28, 2020, accepted June 26, 2020, date of publication June 30, 2020, date of current version July 20, 2020.

Digital Object Identifier 10.1109/ACCESS.2020.3006015

Beam-Sweeping Design Based on Nearest Users Position and Beam in 5G mmWave Networks

STEFANO TOMASIN[1,2], (Senior Member, IEEE), CHRISTIAN MAZZUCCO[3], DANILO DE DONNO[3], AND FILIPPO CAPPELLARO[4]

[1]Department of Information Engineering, University of Padova, 35131 Padova, Italy
[2]Consorzio Nazionale Interuniversitario per le Telecomunicazioni (CNIT), Padova Research Unit, University of Padova, 35131 Padova, Italy
[3]Milan Research Center, Huawei Technologies Italia S.r.l., 20147 Milan, Italy
[4]Sielte, 35129 Padova, Italy

Corresponding author: Stefano Tomasin (tomasin@dei.unipd.it)

This work was supported by the Ministero dell'Istruzione, dell'Università e della Ricerca (MIUR) (Italian Minister for Education) through the initiative Departments of Excellence (Law 232/2016).

ABSTRACT The *beam sweeping* procedure estimates the beamforming directions, or *beams*, to be used for downlink millimeter-wave cellular transmissions to an incoming user entering the cell. We propose three new approaches for the choice of the sequence by which beams are explored (the *beam-search sequence*), in order to reduce the average time to find the directions. The proposed methods exploit a) the correlation among angles of departure of the incoming user and its nearest, already connected user, and b) the position of both the incoming and its nearest user. For point a), the nearest-neighbor-beam search method starts from the beam of the nearest user, and then explores other beams, with directions progressively farther away (in the angular domain) from the first beam. In the beam-and-angle search, the beam-search sequence is optimized by exploiting the knowledge of both users' position and the nearest-user beam. We also propose the simplified beam-and-angle search, which still exploits the nearest-user information, although in a suboptimal and simpler fashion. Based on the channel model of the 3rd generation partnership project, we analytically design the optimal beam-and-angle search sequence. We assess the performance of the proposed solutions, in terms of their average discovery time, also in comparison with existing approaches.

INDEX TERMS Land mobile radio cellular systems, MIMO systems, millimeter wave radio communication.

I. INTRODUCTION

The fifth-generation (5G) of cellular systems will use millimeter waves (mmWave) to achieve ambitious data-rate targets. The strong attenuation incurred by mmWave requires the use of multiple antennas: in downlink, the base station has to direct its transmission toward the user. Therefore, when an incoming user enters a cell, the base station has to find the beamforming direction (named *beam*), by using a suitable *beam sweeping*, or initial access, procedure [1]: the base station transmits pilot signals known to the receiver with specific beams, until the incoming user detects one of them. Each beam covers an angular sectors on the plane,[1] and all the beams cover the whole space. The order by which beams are explored (i.e., the *beam-search sequence*) has impact on the time needed to complete the beam-sweeping procedure. For example, in the random beam search, also denoted as exhaustive search [2], the beam-search sequence is a random permutation of the beams, not related to the specific context (cell geometry, user positions,...).

Over the recent years, various approaches have been proposed to speed up beam sweeping. The research evolved around two types of solution: autonomous search and context-aware search. The autonomous search utilizes only the channel between the incoming user and the base station, without the support of other information. The latter type exploits instead context information, e.g., the user position, or the user-base station channel in another frequency band (e.g., in a non-standalone scenario, wherein a long-term evolution (LTE) link has been established before the mmWave link). About autonomous search, in [3] various techniques are compared, including random-beam and hierarchical searches. Among other solutions, we recall that of [4], wherein the base station periodically transmits pilot

The associate editor coordinating the review of this manuscript and approving it for publication was Anandakumar Haldorai.

[1]More in general, a beam covers a solid angle in the three-dimensional space. Here we ignore the vertical dimension, thus focusing on a two-dimensional scenario.

signals in random directions and the user detects pilots by a generalized likelihood ratio test. In [5], four different non-context-aware protocols, variations of the exhaustive search, are studied under several performance metrics. Special solutions have also been devised for hybrid beamforming [6]. In a railway scenario, positioning and beam sweeping are jointly performed [7]. In [8] it is proposed that a WiFi router transmits a signal in multiple carefully designed directions simultaneously, obtaining a discovery time growing only logarithmically with the number of beams. Lastly, the gradient of the channel gain is exploited in [9], thus halving the average discovery time with respect to the random search.

In this paper, we focus on the context-aware search. Various context-aware approaches have been proposed. A learning approach is investigated in [10], where the statistics of the most used beams is collected and used to design the beam-search sequence. A machine learning model is introduced in [11], that trains a support vector machine for approximating the function that maps the geolocation information of the incoming user to the beam index. A cell-discovery procedure that exploits the knowledge of the incoming user position in a non-standalone configuration is investigated in [12]. The beam-search sequence can also be found by machine learning techniques applied on past beam-sweeping procedures [13], [14]. The statistics of the time and typical paths of entrance into the cell can also be exploited, in order to search the most used beams more often [15], [16]. In a non-standalone scenario, a context-aware solution based on feeding location information to a support vector machine is studied in [17]. The case study of [18] is wireless backhaul communications, where wind flows or ground vibrations move the antennas: the information on the local displacement is exploited to make faster the initial access. The estimated microwave channel using a pre-existing link is exploited in [19] to reduce the space of search with a deep learning method. Surveys on the design of beam-sweeping procedures are [20]–[23].

Despite the large literature on context-aware search approaches, an information that has been scarcely exploited until now is the beam and the position of *other users* already connected to the base station on mmWave and near to the incoming user. Indeed, a vast literature [24]–[28] has shown that nearby users experience highly correlated downlink channels. The spatial consistency of the channel is found also at mmWave, as shown by experiments [24]. Note that the spatial consistency refers to reflections due to static objects (thus related to shadowing) [25]–[27]: at mmWave, it spans tens of meters [28] and should not be confused with the small-scale spatial correlation, associated to fading, which is of only tens of centimeters. Indeed, in [29] it is proposed to create a database of propagation characteristics in the cell, and beam sweeping is optimized based on the information on points around the incoming user. While still exploiting the spatial correlation, we propose three new approaches for fast beam sweeping. In particular, in the nearest-neighbor-beam search, we first explore the beam of the nearest user, and then other beams, moving gradually away from the first one. In the beam-and-angle search, the beam-search sequence is based also on the knowledge of both the incoming user and its nearest user. We finally propose the simplified beam-and-angle search, which still exploits the nearest-user information, but in a suboptimal and simpler fashion. The approach is similar to [29], however a) we do not need a database, b) we do not rely on the time-invariance of channel characteristics, and c) our approach is based on the statistical channel model, rather than collected data. Moreover, we have to design the entire beam-search sequence for the beam-and-angle search, based on the entire channel statistics. To this end, we provide the analytical design of the optimal sequence based on the spatially-consistent 3rd generation partnership project (3GPP) channel model [28]. This derivation will also be useful for the performance evaluation of the proposed techniques. We compare the nearest-neighbor-beam, the beam-and-angle, and the simplified beam-and-angle searches, with the random beam search [2], the solution of [12], based on the incoming user position, and the autonomous search method [9], showing the advantage of our novel approaches. With respect to the other existing literature, our approach combines the statistical information of the beam where most probably the incoming user is found (similarly to [10], [14]–[17]) with the instantaneous information about the nearest user (similarly to [12], [20], [30]), while existing solutions do not merge the two pieces of information.

The rest of the paper is organized as follows. Section II introduces the system model, including the reference statistical channel model as defined by 3GPP, and a short description of three reference beam-search sequence design methods, namely the random beam search, the line-of-sight (LOS) angle search [12], and the single-peak search of [9]. The new beam-search sequence designs, based on information on the nearest user, are described in Section III, and the statistics required for this design are obtained in Section IV. In Section V we discuss numerical results, comparing the proposed solutions with the reference approaches of Section II. Lastly, in Section VI we draw some conclusions.

II. SYSTEM MODEL

We consider one cell of a cellular system, with a base station serving N_{UE} users already connected by mmWave links. Without loss of generality, we assume that the base station is located at position $(0, 0)$. For simplicity, we consider a two-dimensional scenario, ignoring the vertical dimension. A downlink communication from the base station to a user is possible if the base station focuses the transmission towards a specific angular sector, by beamforming. We assume that the base station uses a codebook of N_S beamformers, illuminating non-overlapping angular sectors of $\nu = 360°/N_S$ degrees each,[2] i.e., the angular sectors are

$$[(s-1)\nu, s\nu), \quad s = 1, \ldots, N_S. \tag{1}$$

[2]Note that here, following the notation of [28], we express all angles in degrees.

Indeed, this is a simple approach, while more sophisticated solutions, e.g., using hierarchical beam sweeping, may include angular sectors with different widths. Most of the results reported here will still hold even for more complex solutions, with suitable adaptations, although a comprehensive investigation is left for a future study. Each angular sector is also denoted as *beam*, and identified by its index s.

We now focus on the entrance of a new user (the *incoming user*) into the cell. Considering a non-standalone scenario [23], the incoming user first establishes a connection with the base station at microwave frequencies, using the LTE standard procedure. Then, the user activates a connection at mmWave frequencies, according to the 5G standard: to this end, the base station has to determine the beam s, to be used for downlink mmWave transmission. The focus of this paper is the procedure for determining the correct beam s, also denoted as initial access or *beam sweeping*.

A. BEAM-SWEEPING PROCEDURE

For beam-sweeping, the 3GPP provides that the base station transmits a sequence of pilot signals (known by the user), using different beams in sequence [31]. The transmission of each pilot signal takes the same time, denoted as *slot*. In particular, the *beam-search sequence* is

$$s_1, s_2, \ldots, s_{N_S}, \tag{2}$$

with $s_i \in \{1, \ldots, N_S\}$, where s_i denotes the beam explored in time slot i.

During the beam-sweeping procedure, the incoming user correlates the received signal with the known pilot signal.[3] Let R_s be the modulus square of the correlation output, when the base station uses beam s. If $R_s > \bar{R}$, with $\bar{R}$ a suitable threshold, then beam s is selected to establish the new mmWave link, the beam-sweeping process is terminated, and the incoming user is *discovered*. Clearly, the choice of the beam-search sequence impacts the discovery time, i.e., the number of slots needed to discover the incoming user.

B. BEAMS AND ANGLES OF DEPARTURE

According to the channel model of downlink mmWave transmissions, the pilot signal propagates through M rays from the base station to the incoming user, either on a LOS path or through reflections on objects surrounding the two devices. Ray m, $m = 1, \ldots, M$, is characterized by an *angle of departure* $\phi_m(x_1, y_1)$ from the base station to the incoming user at position (x_1, y_1). We assume here that $R_s > \bar{R}$, $s = 1, \ldots, N_S$, thus the incoming user is discovered for any beam s that includes in its angular sector the angle of departure of any ray, i.e., for any s and $m \in \{1, \ldots, M\}$, such that

$$\phi_m \in [(s-1)\nu, s\nu)\,. \tag{3}$$

[3] The user will perform multiple beamforming combiners on the received signal, in order to focus on the best angle of arrival of the signal. This procedure does not impact the discovery time of the user, thus we are not interested in the angle of arrival of the signal received by users.

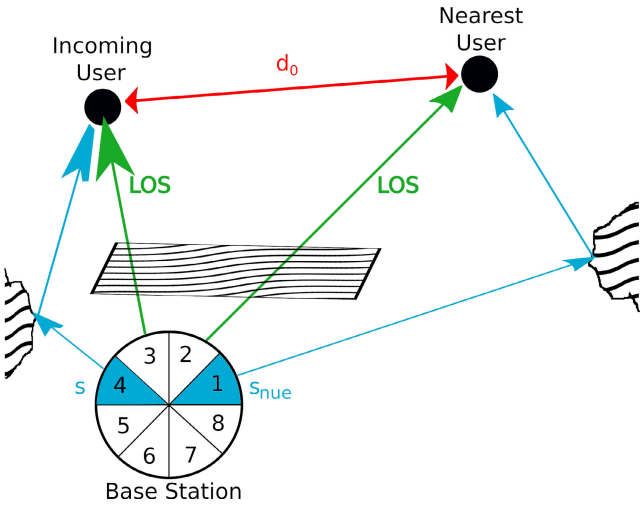

FIGURE 1. Considered propagation scenario. s is the beam used for the incoming user, and s_{NUE} is the beam used for the nearest user.

Fig. 1 shows the considered scenario, with base station, users, LOS lines, active beams, and one signal reflection ($M = 2$). In particular, beyond the incoming user, we have indicated its nearest user, also simply denoted as *nearest user*, that will provide context information for beam sweeping, as detailed in the following. In the figure, the LOS paths between the base station and the users are obstructed, and communication occurs through the reflected paths: the incoming user is discovered with beam $s = 4$, while the nearest user is discovered with beam $s_{NUE} = 1$.

In Section II-C we will provide a description of the statistical model of the angle of departure $\phi_m(x_1, y_1)$. We will highlight that the angle of departures $\phi_m(x_1, y_1)$ and $\phi_m(x_2, y_2)$ for two users at positions (x_1, y_1) and (x_2, y_2) are correlated [24]–[28], since reflections of the rays reaching the two users typically occur on the same objects. In the rest of the paper we will exploit this correlation (also denoted as *spatial consistency* of the channel model) to choose the beam-search sequence (2), in order to reduce the average discovery time. To this end, we will assume that the base station knows both the physical position and the beam of each of the N_{UE} already connected users. This is achieved by letting the incoming user to establish its position (by either satellite or network positioning services), and then send it to the base station through the microwave link (recall we are operating in non-standalone mode); all users will also update their reported positions as they move in the cell, possibly using the mmWave link, once established.

C. ANGLE OF DEPARTURE MODEL OF DOWNLINK SIGNAL

We focus on the spatially-consistent 3GPP model of the downlink angle of departure [28, Proc. B, Section 7.6.3.2], where the channel has either $(M-1)$ or M rays, in LOS or non-LOS (NLOS) conditions, respectively.[4]

[4] Here we consider only the first cluster, as it is characterized by the largest gains [28].

For a user in position (x, y), $\delta(x, y)$ is its distance to the base station. Let $\lambda(x, y) = 1$, if the user is in LOS condition, and $\lambda(x, y) = 0$, if the user is in NLOS condition. Each variable $\lambda(x, y)$ is a Bernoulli random variable with probability of being in LOS [28]

$$P_{\text{LOS}}(x, y) = \begin{cases} 1 & \delta(x, y) \le \delta_0, \\ \dfrac{\delta_0}{\delta(x, y)} + \left(1 - \dfrac{\delta_0}{\delta(x, y)}\right) e^{-\frac{\delta(x,y)}{2\delta_0}} & \delta(x, y) > \delta_0, \end{cases} \tag{4}$$

where $\delta_0 = 18$ m.[5]

The angle of departure for a downlink transmission is modeled as the sum of three components: the LOS angle of departure, the cluster angle of departure, and a random component. The LOS angle of departure is $\phi_{LOS}(x, y) = \text{atan2}(x, y)$, where atan2$(\cdot, \cdot)$ is the *2-argument* arc-tangent. The cluster angle of departure is $c_{ASD}(x, y)\xi_m$, where ξ_m is given in [28, Table 7.5-3] and $c_{ASD}(x, y)$ is a deterministic function of $\lambda(x, y)$ given in [28, Table 7.5-6]. The random component is

$$\gamma(x, y) = \begin{cases} \theta(x, y) \cdot u(x, y), & \text{if } \lambda(x, y) = 0, \\ 0 & \text{if } \lambda(x, y) = 1, \end{cases} \tag{5}$$

with $u(x, y) \sim \mathcal{U}(-1, 1)$, i.e., uniformly distributed in the interval $[-1, 1]$, and the azimuth spread of departure angle $\theta(x, y)$ is defined in [28, Table 7.5-6] as a deterministic function of $\lambda(x, y)$.

Therefore, the angle of departure of ray m in point (x, y) is ($[\cdot]_u$ is the modulo-u operator)

$$\phi_m(x, y) = [\gamma(x, y) + \phi_{LOS}(x, y) + c_{ASD}(x, y)\xi_m]_{360}. \tag{6}$$

The spatial consistency for the angle of departure is obtained by imposing that in positions (x, y) and (x', y') (at distance d), $u(x, y)$ and $\lambda(x, y)$ have a correlation exponentially decaying with d (see [28, Table 7.6.3.1-2]), i.e.,

$$\rho_u(d) = \mathbb{E}[u(x, y)u(x', y')] = e^{-\frac{d}{\Delta_u}}, \tag{7}$$

and, for $\delta(x, y), \delta(x', y') > \delta_0$,

$$\rho_\lambda(d) = \mathbb{E}[\lambda(x, y)\lambda(x', y')] = e^{-\frac{d}{\Delta_\lambda}}, \tag{8}$$

where Δ_u and Δ_λ are the correlation distances for the two variables.

D. REFERENCE BEAM-SEARCH SEQUENCE DESIGN

We now summarize three choices for the beam-search sequence (2), namely the random beam search, the LOS-angle search, and the single-peak search.

1) RANDOM-BEAM SEARCH

With the random-beam search, the beam-search sequence is a uniformly random permutation of $[1, \ldots, N_s]$. The random-beam is also denoted as sequential or *exhaustive* search [2].

[5]This definition of LOS probability holds for the urban micro (UMi) scenario, while for the other scenarios of [28], similar expressions hold, and the derivations of the following sections can be easily adapted also to them.

Algorithm 1 Line-of-Sight-Angle Search

Input: $\phi_{LOS}(x_1, y_1)$
Output: Sector sequence $\{s_1, \ldots, s_{N_S}\}$
1 **begin**
2 $\quad s_1 \longleftarrow s_{LOS}$;
3 $\quad i \longleftarrow 1$;
4 $\quad$ **while** $i < N_S$ **do**
5 $\quad\quad i \longleftarrow i + 1$;
6 $\quad\quad s_i \longleftarrow \left[s_1 - 1 + (-1)^i \left\lfloor \frac{i}{2} \right\rfloor\right]_{N_S} + 1$;
7 $\quad$ **end**
8 **end**

2) LINE-OF-SIGHT-ANGLE SEARCH

The line-of-sight-angle [12] search is a context-aware search method, wherein the beam-search sequence starts with $s_1 = s_{LOS}$, i.e., the beam containing the LOS angle between the base station and the incoming user, $\phi_{LOS}(x_1, y_1)$. Then, other beams follow, from the nearest to s_1 to the farthest (in the angular domain). The line-of-sight-angle solution is reported in Algorithm 1. This beam-search sequence design does not require a communication exchange with nearby users but requires the knowledge of the position of the incoming user. Line 6 of Algorithm 1 is a mathematical formulation of the beam-search sequence, starting from the beam closest to s_1, where $\lfloor x \rfloor$ denotes the floor of x.

3) SINGLE-PEAK SEARCH

The single-peak [9] search is an autonomous method, based on the observation that the channel gain resulting from using different beams grows when the beam angular sector gets closer to the angle of departure. Thus, starting from a random beam index s_1, the algorithm iteratively moves to the beam providing the largest gain among the two beams with adjacent angular sectors, having indices $[s_1]_{N_S} + 1$ and $[s_1 - 2]_{N_S} + 1$.

III. NEIGHBOR-ASSISTED INITIAL ACCESS

We propose three new techniques for the design of the beam-search sequence. In the first approach, denoted nearest-neighbor-beam search, the beam-search sequence starts with the beam used for the nearest user, and then other beams progressively away follow. In the second approach, denoted beam-and-angle search, the beam-search sequence minimizes the average discovery time, exploiting the knowledge of both the LOS angle of departure for the incoming user and the beam of the nearest user. Lastly, the simplified beam-and-angle search still exploits the same information of beam-and-angle, although in a suboptimal fashion.

In all cases, we suppose to know both the position and the beam of the nearest user. Note that the positions of users are known to the cellular network since various cellular generations: the nearest user can be easily identified from this information and, since it is assumed to be already connected by a mmWave link, the base station can send its beam over the LTE link of the incoming user. We indicate with (x_1, y_1) the

position of the incoming user, and with (x_2, y_2) the position of the nearest user. Moreover, we indicate with s_{NUE} the beam used for the nearest user, and with d_0 the distance between the nearest user and the incoming user.

A. NEAREST-NEIGHBOR-BEAM SEARCH

With the nearest-neighbor-beam approach, we assume that both the incoming and its nearest user are close enough to have similar propagation conditions, thus it is likely that they can be reached using the same beam. Thus, $s_1 = s_{NUE}$ is the first beam of the beam-search sequence. If the incoming user is not found in beam s_{NUE}, we explore the other beams, starting from those closest to s_{NUE}, still assuming that the angles of departure of the two users are close enough. The nearest-neighbor-beam search solution is reported in Algorithm 2.

Algorithm 2 Nearest-Neighbor-Beam Search

Input: s_{NUE}
Output: Sector sequence $\{s_1, \ldots, s_{N_S}\}$
begin
  $s_1 \longleftarrow s_{NUE}$;
  $i \longleftarrow 1$;
  while $i < N_S$ **do**
    $i \longleftarrow i + 1$;
    $s_i \longleftarrow \left[s_1 - 1 + (-1)^i \left\lfloor \frac{i}{2} \right\rfloor\right]_{N_S} + 1$;
  end
end

Note that nearest-neighbor-beam search is different from the line-of-sight-angle search, as the first method takes into account the possibility that users are in NLOS condition, and attempts to infer the correct beam from the beam of the nearest user.

B. BEAM-AND-ANGLE SEARCH

We merge now the advantages of both the nearest-neighbor-beam and the line-of-sight-angle algorithms, by exploiting a) the position of both incoming and its nearest users, collected into vector $\boldsymbol{\omega} = [x_1, y_1, x_2, y_2]$, and b) the beam of the nearest user, s_{NUE}. With the beam-and-angle search we optimize the entire sequence $s_1, \ldots, s_{N_S}$, with the aim of minimizing the average discovery time.

To this end, we observe that the minimization of the average discovery time is achieved by a beam-search sequence starting with beams with higher probability of finding the incoming user. In formulas, letting $p(s|\boldsymbol{\omega}, s_{NUE})$ be the probability of finding the incoming user in beam s, given $\boldsymbol{\omega}$ and s_{NUE}, the beams are explored with decreasing conditional probability, i.e.,

$$p(s_i|\boldsymbol{\omega}, s_{NUE}) \geq p(s_{i+1}|\boldsymbol{\omega}, s_{NUE}). \tag{9}$$

The resulting beam-and-angle solution is reported in Algorithm 3. Note that this approach requires the knowledge of the probability of finding the user in each beam. In this paper, we analytically derive the conditional probabilities from the 3GPP channel model, as detailed in Section IV. Other approaches may estimate the conditional probability by collected data on the positions and beams used to discover users through an autonomous search method, and then switch to our context-based solution. However, this opportunity is left for future study.

Algorithm 3 Beam-and-Angle Search

Input: $p(k|\boldsymbol{\omega}, s_{NUE}), k = 1, \ldots, N_S$
Output: Sector sequence $\{s_1, \ldots, s_{N_S}\}$
begin
  $\mathcal{W} = \{1, \ldots, N_S\}$;
  $i \longleftarrow 1$;
  while $i \leq N_S$ **do**
    $s_i \longleftarrow \text{argmax}_{s \in \mathcal{W}}\, p(s|\boldsymbol{\omega}, s_{NUE})$;
    $\mathcal{W} \longleftarrow \mathcal{W} \setminus \{s_i\}$;
    $i \longleftarrow i + 1$;
  end
end

C. SIMPLIFIED-BEAM-AND-ANGLE SEARCH

The simplified beam-and-angle search algorithm is a simplified version of the beam-and-angle search, which does not require the knowledge of the conditional probability $p(s|\boldsymbol{\omega}, s_{NUE})$. It is based on the assumption that if the distance between the incoming user and its nearest user, d_0, is small, then they will most probably use the same beam (s_{NUE}), thus being convenient to adopt the nearest-neighbor-beam search algorithm. On the other hand, when the distance between the two terminals is high, the beam of the incoming user is less correlated to the beam of the nearest user: in this case, it is more convenient to adopt the line-of-sight-angle search approach. Therefore, a simple threshold θ_d on distance d_0 is used to switch between the two algorithms. In particular, we set the threshold θ_d so that the selected algorithm (either nearest-neighbor-beam or line-of-sight-angle) minimizes the average discovery time at distance d_0.

The simplified beam-and-angle solution is reported in Algorithm 4.

IV. ALGORITHM DESIGN AND ANALYSIS

For the design of the beam-and-angle algorithm, we exploit $p(s|\boldsymbol{\omega}, s_{NUE})$, the probability of discovering the incoming user with beam s, given the position of the users and the beam used for the discovery of the nearest user, s_{NUE}. We first compute this probability for a single ray ($M = 1$) and given LOS conditions of the two users. Then, we take the average over the LOS conditions, to obtain $p(s|\boldsymbol{\omega}, s_{NUE})$. Lastly, we generalize the analysis to multiple rays ($M > 1$) in Section IV-D.

Algorithm 4 Simplified Beam-and-Angle Search

Input: s_{NUE}, d_0, s_{LOS}
Output: Sector sequence $\{s_1, \ldots, s_{N_S}\}$

```
begin
    if d_0 > θ_d then
        s_1 ⟵ s_LOS;
    else
        s_1 ⟵ s_NUE;
    end
    i ⟵ 1;
    while i < N_S do
        i ⟵ i + 1;
        s_i ⟵ [s_1 + (1/4)(-1)^i (2i + (-1)^i - 1) - 1]_{N_S} + 1;
    end
end
```

A. ANGULAR SECTOR PROBABILITY FOR LOS CONDITIONS AND $M = 1$

We now consider the case of a single ray, $M = 1$, and given LOS conditions $\boldsymbol{\lambda} = [\lambda(x_1, y_1), \lambda(x_2, y_2)] = \boldsymbol{\lambda}' = [\lambda'_1, \lambda'_2]$. Let us define [see (6)]

$$Z_i = \gamma(x_i, y_i) + \phi_{LOS}(x_i, y_i) + c_{ASD}(x_i, y_i)\xi_1, \quad i = 1, 2, \quad (10)$$

so that $\phi_1(x_i, y_i) = [Z_i]_{360}$. For a given value of $\boldsymbol{\lambda}$, $c_{ASD}(x_i, y_i)$, $i = 1, 2$, are deterministic, and the only random variable in (10) is $\gamma(x_i, y_i)$, so that $Z_i \sim \mathcal{U}(\alpha_i, \beta_i)$, with

$$\alpha_i = -\theta(x_i, y_i) + \phi_{LOS}(x_i, y_i) + c_{ASD}(x_i, y_i)\xi_1, \quad (11)$$

$$\beta_i = \theta(x_i, y_i) + \phi_{LOS}(x_i, y_i) + c_{ASD}(x_i, y_i)\xi_1. \quad (12)$$

Note that Z_1 and Z_2 are correlated random variables, whose joint statistics depends only the distance d_0 between the incoming and the nearest user, through the distance-based correlation of $u(x_i, y_i)$ from (7), rather than their exact positions.

From (5) and (6), the probability that the angle of departure of the incoming user is in the angular sector $[a_1, b_1)$, given LOS conditions $\boldsymbol{\lambda} = \boldsymbol{\lambda}'$ and that the angle of departure of the nearest user is in the angular sector $[a_2, b_2)$, is, for $M = 1$,

$$\begin{aligned}\bar{P}(\boldsymbol{\omega}, \boldsymbol{\zeta}, \boldsymbol{\lambda}') &= \mathbb{P}\left[[Z_1]_{360} \in [a_1, b_1) \mid [Z_2]_{360} \in [a_2, b_2), \boldsymbol{\lambda} = \boldsymbol{\lambda}'\right] \\ &= \frac{\mathbb{P}\left[[Z_1]_{360} \in [a_1, b_1), [Z_2]_{360} \in [a_2, b_2) | \boldsymbol{\lambda} = \boldsymbol{\lambda}'\right]}{\mathcal{I}(\alpha_2, \beta_2, a_2, b_2)}, \end{aligned} \quad (13)$$

where $\mathbb{P}[\cdot]$ denotes the probability operator,

$$\begin{aligned}\mathcal{I}(\alpha_2, \beta_2, a_2, b_2) &= \mathbb{P}\left[[Z_2]_{360} \in [a_2, b_2) | \lambda(x_2, y_2) = \lambda'_2\right] \\ &= \frac{\int_{([a_2, b_2) \cap [\alpha_2, \beta_2))_{360}} da}{\beta_2 - \alpha_2}, \end{aligned} \quad (14)$$

and the modulo operation in the set of the integral in (14) means that all points of the set $[a_2, b_2) \cap [\alpha_2, \beta_2)$ are modulo 360.

Since the angles of departure of the incoming and nearest user are exponentially-correlated uniform random variables, we compute the numerator of $\bar{P}(\boldsymbol{\omega}, \boldsymbol{\zeta}, \boldsymbol{\lambda}')$ in (13) by exploiting the generation of the correlated random variables Z_1 and Z_2. In order to obtain the variables, we generate independent zero-mean unitary-variance Gaussian random variables $Y(x, y)$ for all the points (x, y) of a square grid with step Δ_u, and filter them width a two-dimensional filter having impulse response $2 \sin\left[\frac{\pi}{6}\rho_u(d)\right]$ (see [32]), where d is the distance of the filtered points. This operation provides the correlated Gaussian random variables $\{v(x, y)\}$. Then, we perform a nonlinear transformation of $\{v(x, y)\}$, in order to generate the desired uniform random variables Z_1 and Z_2. In particular, since the inverse of the cumulative distribution function (CDF) of the uniform distribution of $Z_i \sim \mathcal{U}(\alpha_i, \beta_i)$ is

$$F_Z^{-1}(a) = a(\beta_i - \alpha_i) + \alpha_i, \quad a \in [0, 1], \quad (15)$$

the statistically correlated random variables $\{Z_i\}$ are obtained as [1]

$$Z_i = (1 - \mathrm{Q}(v(x_i, y_i)))\,(\beta_i - \alpha_i) + \alpha_i, \quad i = 1, 2, \quad (16)$$

where $\mathrm{Q}(\cdot)$ is the Q-function. Then (13) can be written as

$$\begin{aligned}&\bar{P}(\boldsymbol{\omega}, \boldsymbol{\zeta}, \boldsymbol{\lambda}') \\ &= \frac{1}{\mathcal{I}(\alpha_2, \beta_2, a_2, b_2)} \\ &\quad \times \mathbb{P}\{[(1 - \mathrm{Q}(v(x_1, y_1)))(\beta_1 - \alpha_1) + \alpha_1]_{360} \in [a_1, b_1), \\ &\quad [(1 - \mathrm{Q}(v(x_2, y_2)))(\beta_2 - \alpha_2) + \alpha_2]_{360} \in [a_2, b_2)\} \\ &= \frac{1}{\mathcal{I}(\alpha_2, \beta_2, a_2, b_2)} \\ &\quad \times \mathbb{P}\{(1 - \mathrm{Q}(v(x_1, y_1)))(\beta_1 - \alpha_1) + \alpha_1 \\ &\quad \in \bigcup_{k_1} [a_1 + 360k_1, b_1 + 360k_1), \\ &\quad (1 - \mathrm{Q}(v(x_2, y_2)))(\beta_2 - \alpha_2) + \alpha_2 \\ &\quad \in \bigcup_{k_2} [a_2 + 360k_2, b_2 + 360k_2)\}. \end{aligned} \quad (17)$$

By defining

$$c_i(k) = 1 - \frac{b_i + 360k - \alpha_i}{\beta_i - \alpha_i}, \quad f_i(k) = 1 - \frac{a_i + 360k - \alpha_i}{\beta_i - \alpha_i}, \quad (18)$$

we can write (17) as

$$\begin{aligned}&\bar{P}(\boldsymbol{\omega}, \boldsymbol{\zeta}, \boldsymbol{\lambda}') \\ &\quad = \frac{1}{\mathcal{I}(\alpha_2, \beta_2, a_2, b_2)} \\ &\quad \times \sum_{k_1} \sum_{k_2} \mathbb{P}\left[\mathrm{Q}(v(x_1, y_1)) \in [c_1(k_1), f_1(k_1)), \right. \\ &\quad \left. \mathrm{Q}(v(x_2, y_2)) \in [c_2(k_2), f_2(k_2))\right]. \end{aligned} \quad (19)$$

Finally, letting $g_i(k_i) = \mathrm{Q}^{-1}(c_i(k_i))$ and $h_i(k_i) = \mathrm{Q}^{-1}(f_i(k_i))$, we have

$$\begin{aligned}\bar{P}(\boldsymbol{\omega}, \boldsymbol{\zeta}, \boldsymbol{\lambda}') &= \frac{1}{\mathcal{I}(\alpha_2, \beta_2, a_2, b_2)} \times \sum_{k_1}\sum_{k_2} \mathbb{P}\left[v(x_1, y_1) \in [g_1(k_1), h_1(k_1)), v(x_2, y_2) \in [g_2(k_2), h_2(k_2))\right] \\ &= \frac{1}{\mathcal{I}(\alpha_2, \beta_2, a_2, b_2)} \times \sum_{k_1}\sum_{k_2} \Xi(g_1(k_1), h_1(k_1), g_2(k_2), h_2(k_2), \rho_u(d_0)),\end{aligned} \tag{20}$$

where

$$\begin{aligned}&\Xi(g_1, h_1, g_2, h_2, \rho_u(d_0)) \\ &\quad = \int_{g_2}^{h_2}\int_{g_1}^{h_1} \frac{1}{2\pi\sqrt{1-\rho_u(d_0)}} \\ &\qquad \times \exp\left[-\frac{u_1^2 - 2\rho_u(d_0)u_1u_2 + u_2^2}{2(1-\rho_u(d_0))}\right] du_1 du_2,\end{aligned} \tag{21}$$

is the probability of bivariate correlated normal random variables over a square, which can be computed numerically [33].

The generalization of the computation of $\bar{P}(\boldsymbol{\omega}, \boldsymbol{\zeta}, \boldsymbol{\lambda}')$ to multiple rays ($M > 1$) is given in Section IV-D.

B. LOS STATISTICS

We now aim at computing the probability of being in LOS conditions $\boldsymbol{\lambda}'$, for given user positions $\boldsymbol{\omega}$. First, we observe that both $\lambda(x_1, y_1)$ and $\lambda(x_2, y_2)$ are correlated Bernoulli random variables, and we proceed analogously to the computation of $\bar{P}(\boldsymbol{\omega}, \boldsymbol{\zeta}, \boldsymbol{\lambda}')$, by exploiting their correlated generation. We start from independent zero-mean unitary-variance Gaussian random variables $\{Y'(x, y)\}$ for all (x, y) on a square grid with step Δ_λ, and filter them with a two-dimensional filter having impulse response $H(d)$, to be determined in the following. This provides correlated Gaussian random variables $\{V'(x, y)\}$. Then, $\lambda(x, y)$ is obtained from the inverse CDF of the Bernoulli random variable with parameter $P_{LOS}(x, y)$ from (4), i.e.,

$$\lambda(x, y) = \begin{cases} 1 & \text{if } \delta(x, y) \le \delta_0, \\ 1 & \text{if } \delta(x, y) > \delta_0 \text{ and } V'(x, y) < K_0, \\ 0 & \text{otherwise,} \end{cases} \tag{22}$$

where

$$K_0 = \mathrm{Q}^{-1}\left\{1 - \left[\frac{\delta_0}{\delta(x, y)} + \left(1 - \frac{\delta_0}{\delta(x, y)}\right) e^{-\frac{\delta(x,y)}{2\delta_0}}\right]\right\}. \tag{23}$$

Now, the correlation of the random variables $\lambda(x, y)$ and $\lambda(x', y')$, where (x, y) and (x', y') are at distance d, is (for $\delta(x, y), \delta(x', y') > \delta_0$)

$$\begin{aligned}\rho_\lambda(d) &= \mathbb{E}[\lambda(x, y)\lambda(x', y')] \\ &= \mathbb{P}(V'(x, y) < K_0, V'(x', y') < K_0) \\ &= \Xi(-\infty, K_0, -\infty, K_0, H(d)).\end{aligned} \tag{24}$$

Thus, by setting $\rho_\lambda(d)$ as in (8) and inverting (24) through numerical methods we obtain $H(d)$.

From (22), we observe that, when both the incoming and the nearest users are at distance $\delta(x_1, y_1), \delta(x_2, y_2) \le \delta_0$ from the base station, they are both in LOS condition. If one of the two users is at a distance larger than δ_0 from the base station, it is a Bernoulli random variable with probability (4); if both users are at a distance $\delta(x_1, y_1), \delta(x_2, y_2) > \delta_0$, the statistics of LOS conditions are related to the joint probability of variables $V'(x_1, y_1)$ and $V'(x_2, y_2)$. In particular, the probability $p_{LOS}(\boldsymbol{\omega}, \boldsymbol{\lambda}')$ of being in LOS conditions $\boldsymbol{\lambda}'$ for given user positions $\boldsymbol{\omega}$ is given by (25), on the bottom of the page.

C. COMPUTATION OF $p(s|\omega, s_{NUE})$

The probability that the angle of departure of the incoming user is in angular sector $[a_1, b_1)$, given the positions of the users $\boldsymbol{\omega}$ and that the angle of departure of the nearest user is in angular sector $[a_2, b_2)$, is therefore

$$\begin{aligned}\kappa(\boldsymbol{\omega}, \boldsymbol{\zeta}) &= \mathbb{P}\left[[Z_1]_{360} \in [a_1, b_1) \mid [Z_2]_{360} \in [a_2, b_2)\right] \\ &= \sum_{\boldsymbol{\lambda} \in \mathcal{L}} \bar{P}(\boldsymbol{\omega}, \boldsymbol{\zeta}, \boldsymbol{\lambda}') p_{LOS}(\boldsymbol{\omega}, \boldsymbol{\lambda}'),\end{aligned} \tag{26}$$

where $\mathcal{L} = \{(0, 0), (0, 1), (1, 0), (1, 1)\}$ is the set of all possible LOS conditions for the two users.

Lastly, the angular sector of beam s is given by (3) and the probability of being discovered with beam s, given the users' position and the beam used for of the nearest user, is

$$p(s|\boldsymbol{\omega}, s_{NUE}) = \kappa(\boldsymbol{\omega}, [(s-1)v, sv, (s_{NUE} - 1)v, s_{NUE}v]), \tag{27}$$

for $s = 1, \ldots, N_S$.

$$\begin{aligned}p_{LOS}(\boldsymbol{\omega}, \boldsymbol{\lambda}') &= \mathbb{P}[\boldsymbol{\lambda} = \boldsymbol{\lambda}' | \boldsymbol{\omega}] \\ &= \begin{cases} 1 & \delta(x_1, y_1) \le \delta_0 \text{ and } \delta(x_2, y_2) \le \delta_0, \\ (1 - \lambda_1') - P_{LOS}(x_1, y_1) & \delta(x_1, y_1) > \delta_0 \text{ and } \delta(x_2, y_2) \le \delta_0, \\ (1 - \lambda_2') - P_{LOS}(x_2, y_2) & \delta(x_1, y_1) \le \delta_0 \text{ and } \delta(x_2, y_2) > \delta_0, \\ \Xi(K_0, K_0, \infty, \infty, H(d)) & \delta(x_1, y_1) > \delta_0 \text{ and } \delta(x_2, y_2) > \delta_0, \lambda_1' = \lambda_2' = 1, \\ \Xi(-\infty, K_0, K_0, \infty, H(d)) & \delta(x_1, y_1) > \delta_0 \text{ and } \delta(x_2, y_2) > \delta_0, \lambda_1' \ne \lambda_2', \\ \Xi(-\infty, -\infty, K_0, K_0, H(d)) & \delta(x_1, y_1) > \delta_0 \text{ and } \delta(x_2, y_2) > \delta_0, \lambda_1' = \lambda_2' = 0 \end{cases}\end{aligned} \tag{25}$$

D. GENERALIZATION TO MULTIPLE RAYS

We generalize here the computation of $\bar{P}(\boldsymbol{\omega}, \boldsymbol{\zeta}, \boldsymbol{\lambda}')$ to the case of multiple rays, i.e., $M > 1$. Let $\phi_m(x_i, y_i) = [Z_{i,m}]_{360}$, where

$$Z_{i,m} = Z_i + c_{ASD}(x_i, y_i)(\xi_m - \xi_1). \tag{28}$$

We now compute the probability that any of the M angles of departure of the incoming user falls into the angular sector $[a_1, b_1)$, given that any of the M angles of departure of the nearest user falls into the angular sector $[a_2, b_2)$, and given LOS conditions $\boldsymbol{\lambda} = \boldsymbol{\lambda}'$, that do not depend on the rays. We then have

$$\bar{P}(\boldsymbol{\omega}, \boldsymbol{\zeta}, \boldsymbol{\lambda}') = \mathbb{P}\left[\bigcup_{m=1}^{M} \left\{[Z_{1,m}]_{360} \in [a_1, b_1)\right\} \mid \bigcup_{m=1}^{M} \left\{[Z_{2,m}]_{360} \in [a_2, b_2)\right\}, \boldsymbol{\lambda} = \boldsymbol{\lambda}'\right]. \tag{29}$$

First, by defining the sets, for $i = 1, 2$,

$$\mathcal{F}_i = \bigcup_{k} \bigcup_{m=1}^{M} [a_i + c_{ASD}(x_i, y_i)(\xi_m - \xi_1) + 360k, \; b_i + c_{ASD}(x_i, y_i)(\xi_m - \xi_1) + 360k], \tag{30}$$

inserting (28) and (30) into (29) we obtain

$$\bar{P}(\boldsymbol{\omega}, \boldsymbol{\zeta}, \boldsymbol{\lambda}') = \mathbb{P}\left[Z_1 \in \mathcal{F}_1 \mid Z_2 \in \mathcal{F}_2, \boldsymbol{\lambda} = \boldsymbol{\lambda}'\right]. \tag{31}$$

In general, intervals $[a_i + c_{ASD}(x_i, y_i)(\xi_m - \xi_1) + 360\ k$, $b_i + c_{ASD}(x_i, y_i)(\xi_m - \xi_1) + 360\ k]$ may overlap for different values of k and m. Still, $\mathcal{F}_i$ can be rewritten as the union of disjoint segments as

$$\mathcal{F}_i = \bigcup_{m} [\tilde{a}_{i,m}, \tilde{b}_{i,m}), \quad i = 1, 2, \tag{32}$$

where $[\tilde{a}_{i,m}, \tilde{b}_{i,m}) \cap [\tilde{a}_{i,m'}, \tilde{b}_{i,m'}) = \emptyset$ for $m \neq m'$. By using the properties of probabilities over disjoint events we have

$$\begin{aligned}\bar{P}(\boldsymbol{\omega}, \boldsymbol{\zeta}, \boldsymbol{\lambda}') &= \sum_{m} \mathbb{P}\left[Z_1 \in [\tilde{a}_{1,m}, \tilde{b}_{1,m}) \mid Z_2 \in \mathcal{F}_2, \boldsymbol{\lambda} = \boldsymbol{\lambda}'\right] \\ &= \frac{1}{\sum_{m'} \mathcal{I}(\alpha_2, \beta_2, \tilde{a}_{2,m'}, \tilde{b}_{2,m'})} \\ &\quad \times \sum_{m=1}^{\tilde{M}} \sum_{m'} \mathbb{P}\left[Z_1 \in [\tilde{a}_{1,m}, \tilde{b}_{1,m}), Z_2 \in [\tilde{a}_{2,m'}, \tilde{b}_{2,m'}) \mid \boldsymbol{\lambda} = \boldsymbol{\lambda}'\right].\end{aligned} \tag{33}$$

Then, the probabilities in (33) can be computed by following the steps of Section IV-A.

V. NUMERICAL RESULTS

We consider a circular cell centered on the base station, and the incoming user is on the circle. The main parameters of the simulated UMi channel model [28] are reported in Table 1. We compare the performance of our proposed nearest-neighbor-beam (NNB), beam-and-angle (BA), and simplified beam-and-angle (SBA) search methods with the literature random-beam (RNB), line-of-sight-angle (LOSA), and single-peak (SP) search methods. In particular, for the SP search method we consider a base station equipped with N_S antennas, using a discrete-Fourier-transform beamformer, so that the channel gain when using beam s, $s = 1, \ldots, N_S$, is

$$G(s) = \left| \sum_{k=0}^{N_S - 1} e^{-2\pi j \frac{(s-1)k}{N_S}} e^{jk(\phi_m(x,y) - \nu/2)} \right|. \tag{34}$$

TABLE 1. Parameters of the channel model.

Parameter	Notation	Value
Carrier frequency	f_c	30 GHz
Number of beams	N_S	64
Beam width	ν	$360°/64$
Cell radius	r	150 m
Number of rays	M	1
Angle dep. corr. distance	Δ_u	12 m LOS / 15 m NLOS
LOS correlation distance	Δ_λ	50 m

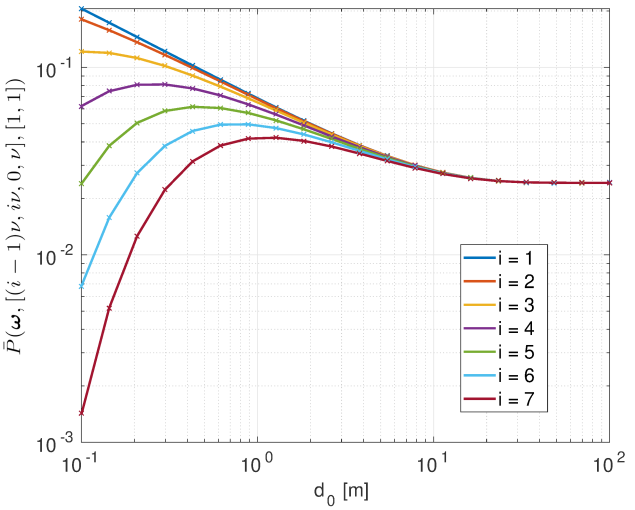

FIGURE 2. Analytical (solid lines) and simulated (crosses) values of $\bar{P}(\boldsymbol{\omega}, [(i-1)\nu, i\nu, 0, \nu], [1, 1])$, as a function of distance d_0.

A. ANGULAR SECTOR PROBABILITY

First, we consider a single-ray scenario, wherein the nearest user is on the line between the base station and the incoming user, at distance d_0 from the incoming user, and both users are in LOS conditions. Without loss of generality, the position of the nearest user is such that $s_{NUE} = 1$. Fig. 2 shows $\bar{P}(\boldsymbol{\omega}, [(i-1)\nu, i\nu, 0, \nu], [1, 1])$ as a function of d_0 and $i = 1, \ldots, N_S - 1$, computed by both analysis and simulation. We observe the perfect correspondence of analytical and simulated results. Due to the correlation, the probability is higher for small values of i, i.e., for beams closer to the beam

of the nearest user, as expected. Moreover, as the distance grows, the probability tends to $1/N_S = 1.6 \cdot 10^{-2}$ for all beams, as the beams of the incoming and the nearest users become independent, and they are uniformly distributed.

B. AVERAGE DISCOVERY TIME VERSUS DISTANCE

Fig. 3 shows the conditional average discovery time $\mathbb{E}[\tau|d_0]$, as a function of the distance d_0, for the same user positions of the previous section. We consider here also random LOS conditions for both users.

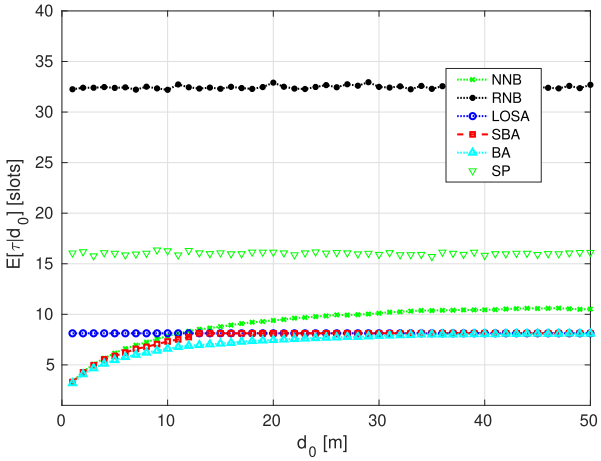

FIGURE 3. Average discovery time as a function of the distance d_0 between the incoming user and the nearest user.

The average discovery time is independent of d_0 for the RNB search. Indeed, since the RNB search selects uniformly at random a permutation of the beam indices, the average discovery time is

$$\mathbb{E}[\tau] = \frac{N_S}{2}. \tag{35}$$

The SP search instead, starting from a random beam, moves to the adjacent beam providing the higher channel gain, until reaching its maximum, thus its average discovery time is $\mathbb{E}[\tau] = \frac{N_S}{4}$.

Since the LOSA search does not exploit any information on the nearest user, its average discovery time is also independent of d_0, and still considerably smaller than the average discovery time or the RNB search method.

Instead, the NNB search algorithm outperforms both LOSA and RNB searches when the two users are closer than 12 m. Indeed, in this range the average discovery time of both NNB and SBA are similar to that of the optimal BA search. Instead, for devices at higher distance, the LOSA approach outperforms NNB. The sub-optimal SBA search instead performs very close to the optimal BA approach in the whole range of distances.

C. EFFECT OF THE NUMBER OF USERS IN THE CELL

We now evaluate the average discovery time as a function of the number of users already present in the cell, N_{UE}. The N_{UE} users are uniformly randomly dropped inside the cell, while the incoming user is still on the circle of the cell border.

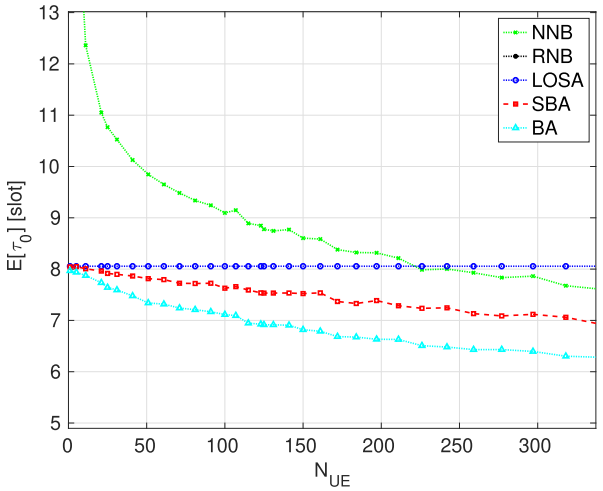

FIGURE 4. Average discovery time as a function of N_{UE}, the number of users in the cell.

Fig. 4 shows the average discovery time as a function of N_{UE}. The average discovery time of the LOSA search is clearly independent of the number of users already present in the cell. We do not report the performance of both RNB and SP search, since their average discovery time is 32 and 16 slots, respectively, which are out of range in the figure. The NNB search shows a higher average discovery time than the LOSA search for $N_{UE} < 170$, while it outperforms the two reference methods for a higher number of N_{UE}. The average discovery time of both SBA and BA instead is always smaller than that of the LOSA search, and their performance improves as the number of users increases. Indeed, for a larger number of users the average distance from nearest user is reduced, thus increasing correlation between the beams of the nearest and incoming users.

D. CDF

We now examine the CDF of the discovery time τ, i.e., $\mathbb{P}[\tau \leq \tau_0]$.

Fig. 5 shows the CDF of the discovery time τ for a distance $d_0 = 5$ m between the incoming and the nearest user. For RNB, SP, and LOSA, τ is a uniformly distributed random variable, thus providing a linearly increasing CDF. For the nearest-neighbor search methods instead, the CDF is non-linear, and we observe that it is higher for each τ_0, thus beam-sweeping is faster. In particular, we observe that $\mathbb{P}[\tau \leq 20] = 0.9$, while for the LOSA search the same probability is reached for $\tau < 28$. This further confirms that the incoming user is discovered faster with the proposed methods than with existing ones.

Fig. 6 shows the CDF of the discovery time τ for a distance $d_0 = 10$ m. As the distance increases, the correlation between the beams of the nearest and incoming users decreases, thus increasing the discovery time. Moreover, we observe that the

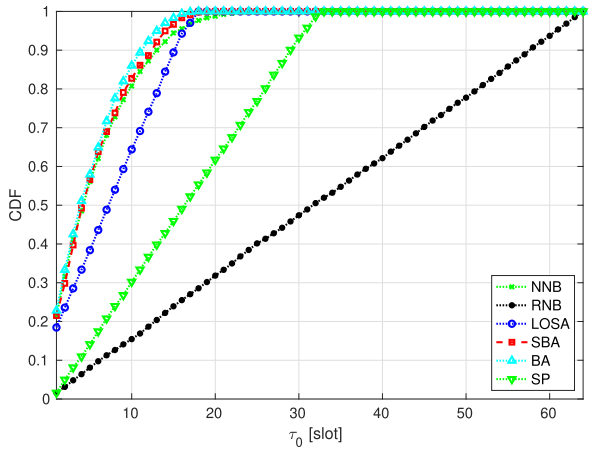

FIGURE 5. CDF of the discovery time τ for distance $d = 5$ m between the nearest user and the incoming user.

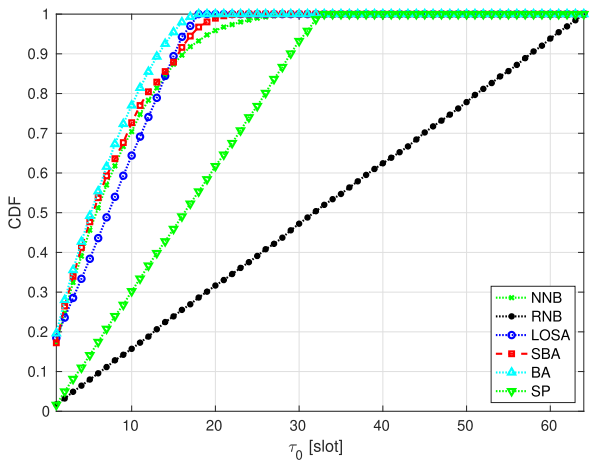

FIGURE 6. CDF of the discovery time τ for distance $d = 10$ m between the nearest user and the incoming user.

NNB search is more sensitive to the reduction of correlation with respect to BA and SBA techniques, as its CDF is now shifted more to the right. Also, overall the performance of the nearest-neighbor searches becomes closer to that of the LOSA search.

Fig. 7-9 show the CDF of the discovery time τ for different numbers N_{UE} of users uniformly distributed in the cell. For a small number of users ($N_{UE} = 5$, Fig. 7), the BA, SBA, and LOSA search methods all perform similarly, and consistently better than the RNB search. With a small probability, the NNB method may perform worse than the SP search, although we note that the two methods could be merged, by considering as initial sector the nearest-neighbor beam sector, and then performing the gradient search according to the SP approach. The NNB search methods, while still outperforming both the RNB and the SP searches, explore more beams. In this case, the exploitation of the LOS component is important, as, due to the small number of users, the information on the nearest user is not very useful. As N_{UE} increases, the nearest user becomes typically closer to the incoming user, thus providing more useful information on the beam to be used. Indeed, for a higher number of users ($N_{UE} = 125$, Fig. 8) the NNB search method has an average

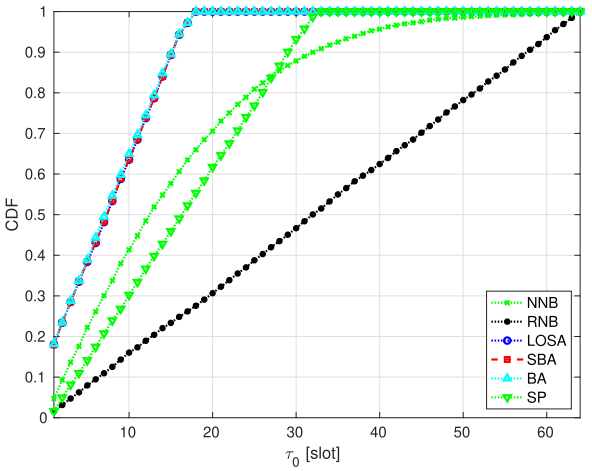

FIGURE 7. CDF of the discovery time τ for $N_{UE} = 5$.

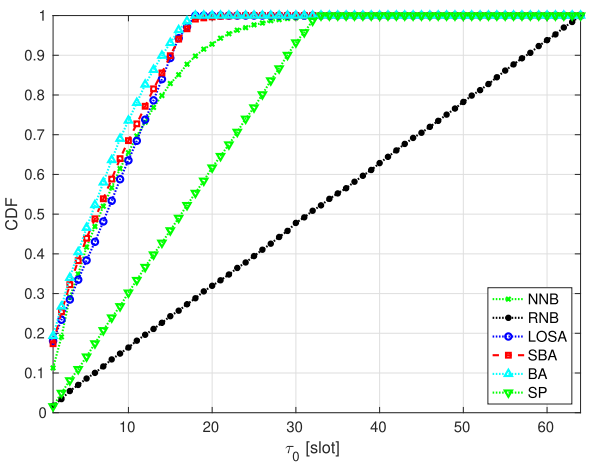

FIGURE 8. CDF of the discovery time τ for $N_{UE} = 125$.

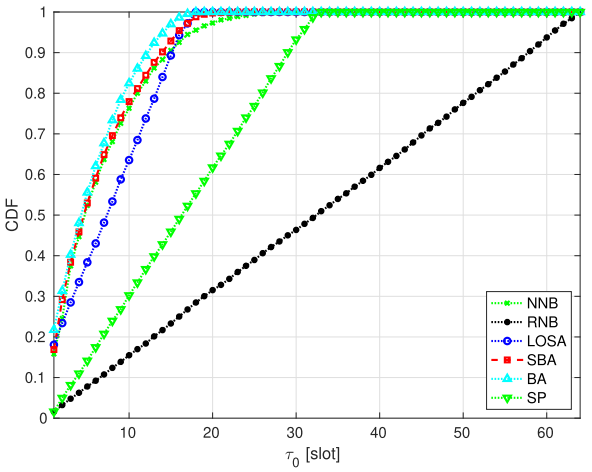

FIGURE 9. CDF of the discovery time τ for $N_{UE} = 625$.

discovery time closer to that of the optimal BA approach, significantly outperforming both the RNB and the SP searches. This effect is further highlighted for an even larger number of users ($N_{UE} = 625$, Fig. 9), where we note that the nearest-neighbor search methods significantly outperform the LOSA search method, that does not exploit this additional information.

VI. CONCLUSIONS

This manuscript has presented three new beam-sweeping methods, based on the context information of the user nearest to the incoming user. In particular, our solutions exploit the information on the beam of the nearest user and its distance from the incoming user, yielding a consistently lower discovery time. We also exploit the full statistics (i.e., the CDF) of the conditional probability of discovering the user with a beam, given the positions of the users. We presented analytical and numerical simulation results for various numbers of rays and users in the cell and conclude that the proposed techniques significantly reduce the average discovery time with respect to three reference beam-sweeping schemes. Finally, we were able to decrease the scanning time by both optimal and suboptimal, less complex, solutions, based on the 3GPP channel model.

REFERENCES

[1] *NR Physical Channels and Modulation*, Standard 3GPP, TS 38.211 V15.4.0, 2018.
[2] C. Jeong, J. Park, and H. Yu, "Random access in millimeter-wave beamforming cellular networks: Issues and approaches," *IEEE Commun. Mag.*, vol. 53, no. 1, pp. 180–185, Jan. 2015.
[3] M. Giordani, M. Mezzavilla, C. N. Barati, S. Rangan, and M. Zorzi, "Comparative analysis of initial access techniques in 5G mmWave cellular networks," in *Proc. Annu. Conf. Inf. Sci. Syst. (CISS)*, Mar. 2016, pp. 268–273.
[4] C. N. Barati, S. A. Hosseini, S. Rangan, P. Liu, T. Korakis, S. S. Panwar, and T. S. Rappaport, "Directional cell discovery in millimeter wave cellular networks," *IEEE Trans. Wireless Commun.*, vol. 14, no. 12, pp. 6664–6678, Dec. 2015.
[5] Y. Li, J. G. Andrews, F. Baccelli, T. D. Novlan, and C. J. Zhang, "Design and analysis of initial access in millimeter wave cellular networks," *IEEE Trans. Wireless Commun.*, vol. 16, no. 10, pp. 6409–6425, Oct. 2017.
[6] D. De Donno, J. Palacios, and J. Widmer, "Millimeter-wave beam training acceleration through low-complexity hybrid transceivers," *IEEE Trans. Wireless Commun.*, vol. 16, no. 6, pp. 3646–3660, Jun. 2017.
[7] J. Talvitie, T. Levanen, M. Koivisto, T. Ihalainen, K. Pajukoski, and M. Valkama, "Positioning and location-aware communications for modern railways with 5G new radio," *IEEE Commun. Mag.*, vol. 57, no. 9, pp. 24–30, Sep. 2019.
[8] H. Hassanieh, O. Abari, M. Rodriguez, M. Abdelghany, D. Katabi, and P. Indyk, "Fast millimeter wave beam alignment," in *Proc. Conf. ACM Special Interest Group Data Commun.*, Aug. 2018, pp. 432–445.
[9] I. Aykin and M. Krunz, "Efficient beam sweeping algorithms and initial access protocols for millimeter-wave networks," *IEEE Trans. Wireless Commun.*, vol. 19, no. 4, pp. 2504–2514, Apr. 2020.
[10] A. Capone, I. Filippini, V. Sciancalepore, and D. Tremolada, "Obstacle avoidance cell discovery using mm-waves directive antennas in 5G networks," in *Proc. IEEE 26th Annu. Int. Symp. Pers., Indoor, Mobile Radio Commun. (PIMRC)*, Aug. 2015, pp. 2349–2353.
[11] M. Arvinte, M. Tavares, and D. Samardzija, "Beam management in 5G NR using geolocation side information," in *Proc. 53rd Annu. Conf. Inf. Sci. Syst. (CISS)*, Mar. 2019, pp. 1–6.
[12] F. Devoti, I. Filippini, and A. Capone, "Facing the millimeter-wave cell discovery challenge in 5G networks with context-awareness," *IEEE Access*, vol. 4, pp. 8019–8034, 2016.
[13] R. Zia-ul-Mustafa and S. A. Hassan, "Machine learning-based context aware sequential initial access in 5G mmWave systems," in *Proc. IEEE Globecom Workshops (GC Wkshps)*, Dec. 2019, pp. 1–6.
[14] F. Devoti, I. Filippini, and A. Capone, "MM-wave initial access: A context information overview," in *Proc. IEEE 19th Int. Symp. World Wireless, Mobile Multimedia Networks (WoWMoM)*, Jun. 2018, pp. 1–9.
[15] H. Soleimani, R. Parada, S. Tomasin, and M. Zorzi, "Statistical approaches for initial access in mmWave 5G systems," in *Proc. Eur. Wireless 24th Eur. Wireless Conf.*, May 2018, pp. 1–6.
[16] H. Soleimani, R. Parada, S. Tomasin, and M. Zorzi, "Fast initial access for mmWave 5G systems with hybrid beamforming using online statistics learning," *IEEE Commun. Mag.*, vol. 57, no. 9, pp. 132–137, Sep. 2019.
[17] A. Pan, T. Zhang, and X. Han, "Location information aided beam allocation algorithm in mmWave massive MIMO systems," in *Proc. IEEE/CIC Int. Conf. Commun. China (ICCC)*, Oct. 2017, pp. 1–6.
[18] G. C. Alexandropoulos,"Position aided beam alignment for millimeter wave backhaul systems with large phased arrays," in *Proc. IEEE 7th Int. Workshop Comput. Adv. Multi-Sensor Adapt. Process. (CAMSAP)*, Dec. 2017, pp. 1–5.
[19] M. S. Sim, Y.-G. Lim, S. H. Park, L. Dai, and C.-B. Chae, "Deep learning-based mmWave beam selection for 5G NR/6G with Sub-6 GHz channel information: Algorithms and prototype validation," *IEEE Access*, vol. 8, pp. 51634–51646, 2020.
[20] M. Giordani, M. Mezzavilla, and M. Zorzi, "Initial access in 5G mmWave cellular networks," *IEEE Commun. Mag.*, vol. 54, no. 11, pp. 40–47, Nov. 2016.
[21] M. Giordani, M. Polese, A. Roy, D. Castor, and M. Zorzi, "A tutorial on beam management for 3GPP NR at mmWave frequencies," *IEEE Commun. Surveys Tuts.*, vol. 21, no. 1, pp. 173–196, 1st Quart., 2019.
[22] M. Giordani, M. Polese, A. Roy, D. Castor, and M. Zorzi, "Initial access frameworks for 3GPP NR at mmWave frequencies," in *Proc. 17th Annu. Medit. Ad Hoc Netw. Workshop (Med-Hoc-Net)*, Jun. 2018, pp. 1–8.
[23] M. Giordani, M. Polese, A. Roy, D. Castor, and M. Zorzi, "Standalone and non-standalone beam management for 3GPP NR at mmWaves," *IEEE Commun. Mag.*, vol. 57, no. 4, pp. 123–129, Apr. 2019.
[24] T. S. Rappaport, G. R. MacCartney, S. Sun, H. Yan, and S. Deng, "Small-scale, local area, and transitional millimeter wave propagation for 5G communications," *IEEE Trans. Antennas Propag.*, vol. 65, no. 12, pp. 6474–6490, Dec. 2017.
[25] S. Ju and T. S. Rappaport, "Millimeter-wave extended NYUSIM channel model for spatial consistency," in *Proc. IEEE Global Commun. Conf. (GLOBECOM)*, Dec. 2018, pp. 1–6.
[26] S. Ju and T. S. Rappaport, "Simulating motion—Incorporating spatial consistency into NYUSIM channel model," in *Proc. IEEE 88th Veh. Technol. Conf. (VTC-Fall)*, Aug. 2018, pp. 1–6.
[27] M. Shafi, J. Zhang, H. Tataria, A. F. Molisch, S. Sun, T. S. Rappaport, F. Tufvesson, S. Wu, and K. Kitao, "Microwave vs. millimeter-wave propagation channels: Key differences and impact on 5G cellular systems," *IEEE Commun. Mag.*, vol. 56, no. 12, pp. 14–20, Dec. 2018.
[28] *Study Channel Model for Frequencies From 0.5 to 100 GHz*, Standard 3GPP, TR 38.901 V15.0.0, 2018.
[29] J. C. Aviles and A. Kouki, "Position-aided mm-wave beam training under NLOS conditions," *IEEE Access*, vol. 4, pp. 8703–8714, 2016.
[30] W. B. Abbas and M. Zorzi, "Context information based initial cell search for millimeter wave 5G cellular networks," in *Proc. Eur. Conf. Netw. Commun. (EuCNC)*, Jun. 2016, pp. 111–116.
[31] *NR Physical Layer Procedures for Control*, Standard 3GPP, TS 38.213 V15.4.0, 2018.
[32] S. T. Li and J. L. Hammond, "Generation of pseudorandom numbers with specified univariate distributions and correlation coefficients," *IEEE Trans. Syst., Man, Cybern.*, vol. SMC-5, no. 5, pp. 557–561, Sep. 1975.
[33] Z. Drezner and G. O. Wesolowsky, "On the computation of the bivariate normal integral," *J. Stat. Comput. Simul.*, vol. 35, nos. 1–2, pp. 101–107, Mar. 1990.

STEFANO TOMASIN (Senior Member, IEEE) received the Ph.D. degree in telecommunications engineering from the University of Padova, Italy, in 2003. Since 2005, he has been with the University of Padova. He was on leave at Philips Research, Eindhoven, The Netherlands, in 2002, Qualcomm Research Laboratories, San Diego, CA, in 2004, Polytechnic University, Brooklyn, NY, USA, in 2007, and the Huawei Mathematical and Algorithmic Sciences Laboratory, Paris, France, in 2015. He is currently an Associate Professor with the University of Padova. His current research interests include physical layer security and signal processing for wireless communications, with applications to fifth-generation cellular systems. From 2011 to 2017, he was an Editor of the IEEE TRANSACTIONS OF VEHICULAR TECHNOLOGY, and he has been an Editor the *EURASIP Journal of Wireless Communications and Networking*, since 2011, and the IEEE TRANSACTIONS ON SIGNAL PROCESSING, since 2016. He is an Editor of the IEEE TRANSACTIONS ON INFORMATION FORENSICS AND SECURITY.

CHRISTIAN MAZZUCCO received the Laurea degree in telecommunications engineering from the University of Padova, Italy, in 2003, and the master's degree in information technology from the Politecnico di Milano, in 2004. In 2004, he joined Nokia Siemens Networks, Milan, where he was involved in research on UWB localization and tracking techniques. From 2005 to 2009, he was involved in several projects mainly researching and developing Wimax systems and high-speed LDPC decoders. In 2009, he joined Huawei Technologies, Italy, studying algorithms for high-power amplifiers digital predistortion, phase noise suppression, and MIMO for point-to-point microwave links. He is currently involved in researching phased array processing and the development of mmWave 5G BTS systems.

DANILO DE DONNO received the B.Sc. and M.Sc. degrees *(cum laude)* in telecommunication engineering from the Politecnico di Milano, Italy, in 2005 and 2008, respectively, and the Ph.D. degree in information engineering from the University of Salento, Lecce, Italy, in 2012. He was a Postdoctoral Fellow of the Electromagnetic Lab Lecce (EML2), University of Salento, from 2012 to 2015, and a Postdoctoral Researcher with the IMDEA Networks Institute, Madrid, Spain, from 2015 to 2017. Since July 2017, he has been a Wireless System Engineer with Huawei Technologies, Milan Research Center. His areas of interest include mm-wave communications, with a main research focus on the development of PHY and MAC algorithms for hybrid and full-digital system architectures.

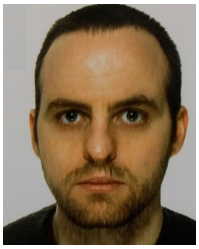

FILIPPO CAPPELLARO was born in Castelfranco Veneto, Italy. He received the M.Sc. degree in telecommunications engineering from the University of Padova, Italy, in 2019. During the master's degree thesis, he worked on cell discovery algorithms for 5G millimeter-wave systems. He is currently employed by Sielte as a Consultant of Vodafone Italia.